Anti-Fermi-Pasta-Ulam energy recursion in diatomic lattices at low energy densities

Sergey V. Dmitriev,[1] Andrey A. Sukhorukov,[2] Anatoly I. Pshenichnyuk,[1] Liya Z. Khadeeva,[1] Albert M. Iskandarov,[1] and Yuri S. Kivshar[2]

[1]*Institute for Metals Superplasticity Problems, Russian Academy of Science, Ufa 450001, Russia*

[2]*Nonlinear Physics Center, Research School of Physics and Engineering, Australian National University, Canberra, Australian Capital Territory 0200, Australia*

(Received 20 May 2009; revised manuscript received 20 July 2009; published 17 September 2009)

We study the dynamics of one- and two-dimensional diatomic lattices with the interatomic Morse potentials for the initial conditions selected at the edge of the Brillouin zone of the dispersion spectrum, when only light atoms are excited with the staggered mode while all heavy atoms remain at rest (the so-called anti-Fermi-Pasta-Ulam problem). We demonstrate that modulational instability of such a nonlinear state may result in *almost periodic* temporal dynamics of the lattice with spatial localization and delocalization of energies. Such a recursion occurs many times with a very slow decay, especially for the initial states with low energy. The energy recursion results in the formation of highly localized, large-amplitude gap *discrete breathers*. For one-dimensional diatomic lattices, we describe the periodic energy recursion analytically for a simple model with the nearest-neighbor interaction and cubic anharmonicity.

DOI: 10.1103/PhysRevB.80.094302 PACS number(s): 05.45.Yv, 63.20.−e

I. INTRODUCTION

At the early age of computers, Fermi, Pasta, and Ulam (FPU) tried to understand the mechanism of energy exchange between different modes of a nonlinear system after excitation of the lowest mode, the longest possible wave in a finite anharmonic chain.[1] They observed an interesting effect when the energy of the excited lowest mode was shared initially between other several modes, but after some time a major part of the energy returned back to the lowest mode. Since that time, the FPU problem is attracting attention of many researchers in connection with the energy localization, soliton formation, chaos, and thermalization.[2] Several decades later, a similar numerical experiment was repeated for the shortest possible wave, for the so-called anti-FPU problem.[3] The kinetics of thermalization of the chain in this case was found to be qualitatively different. At the beginning, spatial localization of energy in the form of discrete breathers (DBs) (Refs. 4–6) was observed. Then a slow degradation of the breathers by means of energy radiation eventually resulted in the thermal equilibrium of the chain. Localization of energy is initiated in the chain via modulational instability, which is a generic phenomenon observed in various physical settings.[7–10] For instance, modulational instability can result in the appearance of the so-called rogue waves.[11] Rigorous results for the modulational instability in diatomic chains were obtained very recently by Doi *et al.*[12]

The analysis of the model equations in the continuum limit derived for the envelope of the modulationally unstable mode at the edge of the Brillouin zone revealed several stages of the energy localization in the chain with hard quartic anharmonicity.[13] According to that study, the first stage of the system evolution is characterized by the emergence of envelope solitons. At the end of the first stage, the DBs with the frequency above the upper edge of the phonon band are formed and they define the subsequent evolution of the system.

In this paper, we study the anti-FPU problem for the case of one- and two-dimensional diatomic anharmonic lattices, when the initial state is selected as a mode at the edge of the Brillouin zone. Such diatomic lattices support DBs with frequencies above or in the gap of the phonon spectrum.[14–16] Gap DBs can also be found, e.g., in the nonlinear dynamics of condensates placed into an optical lattice.[8]

Recent experiments provide evidence of DBs in the lattice dynamics of conventional three-dimensional (3D) materials.[17] Very recently, the gap DBs have been detected experimentally in NaI crystal.[18] In inelastic neutron measurements of the high-temperature lattice excitations in NaI, it was found that in thermal equilibrium at 555 K, an intrinsic mode, localized in three dimensions, occurs at a single frequency near the center of the spectral phonon gap, polarized along [111]. Potential application of DBs in designing a solid-state thermal rectifier has been discussed based on the experimental evidence that DBs can be supported by α-uranium lattice at sufficiently high temperatures.[19]

We demonstrate that modulational instability may result in *almost periodic* spatial localization and delocalization of energy. The energy recursion stage ends with the formation of highly localized, large-amplitude gap DBs. For one-dimensional diatomic lattices, we describe this periodic energy localization/delocalization analytically for a simple model with the nearest-neighbor interactions and cubic anharmonicity.

In order to demonstrate that this is a generic effect, we also study numerically the energy localization in two-dimensional diatomic lattices under the conditions similar to those analyzed for one-dimensional ones. For sufficiently small amplitude of the excited staggered nonlinear state at the edge of the Brillouin zone, we observe the development of periodic in time energy localization/delocalization, similar to the case of one-dimensional lattices. At the later stage, we observe the formation of a few highly localized, large-amplitude DBs. Slow radiation of energy by the DBs at the final stage of the evolution resulted in the subsequent thermal equilibrium of the system.

In our study of the two-dimensional diatomic lattice, we use the Morse potentials taking into account the long-range

interactions. The Morse pair potentials are widely used in molecular-dynamics simulations of solids (see, e.g., Ref. 20 and some recent works[21]), even for metals, for solving the problems where the exact anisotropy of the elastic constants is not important.[22] The Morse potential is rather simple, but, in many cases, it provides much more realistic description of the interatomic interactions than the nearest-neighbor interactions with the simplest types of anharmonicity, typically used in the studies done in the spirit of the nonlinear physics.[12,14–16]

The paper is organized as follows. In Sec. II, we study numerically the dynamics of an unstable staggered mode in one-dimensional diatomic lattices with the Morse interatomic potentials and then develop simplified theory to describe this effect analytically. In Sec. III, we extend our numerical analysis to the case of two-dimensional diatomic lattices and reveal the dynamics qualitatively similar to the one-dimensional lattice. Section IV concludes the paper.

II. ENERGY RECURSION IN A ONE-DIMENSIONAL DIATOMIC CHAIN

A. Model

We consider a diatomic chain with alternating particles of masses m and M (for definiteness we take $m \leq M$). Each particle interacts with its nearest neighbors via the Morse potential taken here in the form

$$U(r) = D\exp\left(-2\alpha\frac{r-r_0}{r_0}\right) - 2D\exp\left(-\alpha\frac{r-r_0}{r_0}\right), \quad (1)$$

where D, α, and r_0 are the parameters and r is the distance between interacting particles. Note that the minimum of the potential $U(r)$ is at $r=r_0$. Let $x_n(t)$ and $X_n(t)$ be, respectively, the coordinates of the light and the heavy particles in the nth periodic cell. Hamiltonian of the system is

$$H = \sum_n \left[\frac{m}{2}\dot{x}_n^2 + \frac{M}{2}\dot{X}_n^2 + U(|x_n - X_{n-1}|) + U(|X_n - x_n|)\right]. \quad (2)$$

Substituting Eq. (1) into Eq. (2) and introducing

$$x_n = 2nh + \tilde{v}_n,$$

$$X_n = (2n+1)h + \tilde{V}_n, \quad (3)$$

where h is the distance between the nearest lattice sites and $\tilde{v}_n$ and $\tilde{V}_n$ are, respectively, the displacements of the light and heavy particles from the corresponding equilibrium positions, we rewrite the Hamiltonian as

$$\tilde{H} = \sum_n \left[\frac{m}{2}\dot{\tilde{v}}_n^2 + \frac{M}{2}\dot{\tilde{V}}_n^2 + \tilde{P}_1 + \tilde{P}_2\right], \quad (4)$$

where

$$\tilde{P}_1 = D\exp(2\tilde{R}_{n-1}) - 2D\exp(\tilde{R}_{n-1}),$$

$$\tilde{P}_2 = D\exp(2\tilde{S}_n) - 2D\exp(\tilde{S}_n), \quad (5)$$

$$\tilde{R}_{n-1} = -\frac{\alpha}{r_0}(\tilde{v}_n - \tilde{V}_{n-1} + h - r_0),$$

$$\tilde{S}_n = -\frac{\alpha}{r_0}(\tilde{V}_n - \tilde{v}_n + h - r_0). \quad (6)$$

Introducing the dimensionless displacements

$$v_n = \frac{\alpha}{r_0}\tilde{v}_n, \quad V_n = \frac{\alpha}{r_0}\tilde{V}_n, \quad (7)$$

dimensionless time, and dimensionless energy

$$\tau = \sqrt{\frac{2D}{m}}\frac{\alpha}{r_0}t, \quad H = \frac{\tilde{H}}{2D}, \quad (8)$$

and the following shorthand notations

$$\delta = \alpha\frac{h-r_0}{r_0}, \quad \varepsilon = \frac{m}{M}, \quad (9)$$

we transform the Hamiltonian to the form

$$H = \sum_n \left[\frac{1}{2}\dot{v}_n^2 + \frac{1}{2\varepsilon}\dot{V}_n^2 + P_1 + P_2\right], \quad (10)$$

where

$$P_1 = \frac{1}{2}\exp(2R_{n-1}) - \exp(R_{n-1}),$$

$$P_2 = \frac{1}{2}\exp(2S_n) - \exp(S_n), \quad (11)$$

$$R_{n-1} = -\delta - v_n + V_{n-1},$$

$$S_n = -\delta - V_n + v_n. \quad (12)$$

One can see that the model essentially has two parameters: the ratio of masses ε and the parameter δ that defines the strain of the lattice. Particularly, for $\delta=0$, one has $h=r_0$, i.e., the lattice spacing coincides with the location of the minimum of the Morse potential which corresponds to the minimum of the potential energy of the chain. The case of $\delta > 0$ (<0) corresponds to tension (compression) of the chain and the potential energy of the chain is higher in these cases than in the case of $\delta=0$.

From the Hamiltonian given by Eq. (10), one can derive the following equations of motion:

$$\ddot{v}_n = e^{2R_{n-1}} - e^{R_{n-1}} - e^{2S_n} + e^{S_n},$$

$$\ddot{V}_n = \varepsilon[e^{2S_n} - e^{S_n} - e^{2R_n} + e^{R_n}]. \quad (13)$$

For sufficiently small displacements v_n and V_n, one can take into account only quadratic anharmonic terms and reduce Eq. (13) to

$$\ddot{v}_n = \alpha(V_{n-1} + V_n - 2v_n) + \beta[(V_{n-1} - v_n)^2 - (v_n - V_n)^2], \quad (14)$$

$$\ddot{V}_n = \varepsilon\alpha(v_n + v_{n+1} - 2V_n) + \varepsilon\beta[(v_n - V_n)^2 - (V_n - v_{n+1})^2], \tag{15}$$

where

$$\alpha = 2e^{-2\delta} - e^{-\delta}, \quad \beta = 2e^{-2\delta} - \frac{1}{2}e^{-\delta}. \tag{16}$$

B. Numerical results

We consider the diatomic chain of N light and N heavy particles (with even N) subjected to the periodic boundary conditions. Initial conditions in Sec. II B are always set assuming that the motion of particles is as follows:

$$v_n(t) = (-1)^n A \sin(\omega t),$$

$$V_n(t) \equiv 0, \tag{17}$$

where A is the amplitude and

$$\omega = \sqrt{2\alpha}, \quad T = 2\pi/\omega \tag{18}$$

are the frequency and the period, respectively. It is readily checked that Eq. (17) satisfies Eq. (14). According to Eq. (17), the light particles oscillate being out of phase with the neighboring light particles and the heavy particles are at rest. It will be demonstrated numerically that the solution Eq. (17) is unstable and this instability results in nontrivial dynamics of the system.

Small perturbation was introduced in the system by shifting the coordinates of heavy atoms at $t=0$, so that instead of the second line in Eq. (17), we actually had $V_n(0)=\Delta_n$, $\dot{V}_n(0)=0$, where Δ_n is a random number homogeneously distributed in the range $[-5\times10^{-8},\ 5\times10^{-8}]$.

In our study, we take in Eq. (17) the amplitudes $A \sim 10^{-2}$. For such small amplitudes, we found that the results obtained from Eqs. (13) and (14) are similar, at least qualitatively, and in the following we report on the results of numerical integration of Eq. (14). The integration was carried out with the use of the Störmer method of order 6.

We calculate the averaged over period T kinetic energies $k_n=\langle \dot{v}_n^2/2\rangle$ and $K_n=\langle \dot{V}_n^2/(2\varepsilon)\rangle$ of the light and heavy particles, respectively. We do monitoring of the time evolution of the following quantities:

$$k = \frac{1}{N}\sum_{n=1}^{N} k_n, \quad K = \frac{1}{N}\sum_{n=1}^{N} K_n,$$

$$L_k = \frac{\sum_{n=1}^{N} k_n^2}{\left(\sum_{n=1}^{N} k_n\right)^2}, \quad L_K = \frac{\sum_{n=1}^{N} K_n^2}{\left(\sum_{n=1}^{N} K_n\right)^2}. \tag{19}$$

The first two quantities are thus the averaged kinetic energies of the light and heavy particles, respectively, while the last two are the localization parameters for the kinetic energies of the light and heavy sublattices.

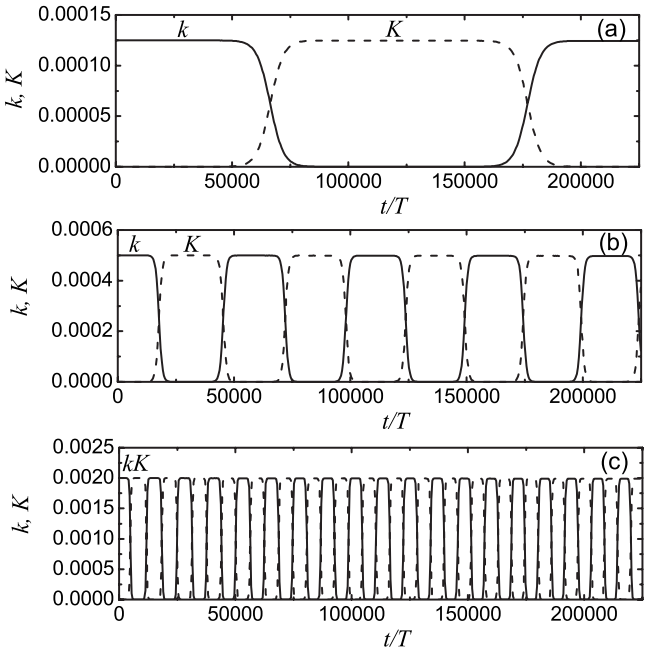

FIG. 1. Time evolutions of k and K for the case of equal masses, $\varepsilon=1$, and for different amplitudes of the excited mode: (a) $A=0.005$, (b) $A=0.01$, (c) $A=0.02$. The result does not depend on N. One can see that for the period of energy exchange between sublattices, one has $S\sim A^{-2}$. Here $\delta=0$.

In this work, we consider the case of undeformed chain by setting $\delta=0$ and study the dynamics of the chains with different ratios of masses ε, different amplitudes of the excited mode A, and different numbers of light and heavy particles N.

The first example is presented in Fig. 1 for the *case of equal masses*, $\varepsilon=1$, and for three different amplitudes: (a) $A=0.005$, (b) $A=0.01$, (c) $A=0.02$. Shown are the averaged kinetic energies of even and odd particles, k and K, respectively, as the functions of time measured in the units of T. In this case, the dynamics is not sensitive to the number of particles and the same picture was observed for $N=2$ and for $N=32$. We do not plot the time evolution of L_k and L_K because no spatial energy localization was observed in the case of $\varepsilon=1$ and the localization parameters were always close to their minimum possible values of $1/N$. As it can be seen from Fig. 1, the total averaged kinetic energy of even and odd particles is practically conserved and it increases with increase in A as A^2. Interestingly, the sublattices of even and odd particles periodically exchange by their kinetic energies with the period of $\sim 10^4T-10^5T$. The period of energy exchange S is proportional to A^{-2}.

Even more interesting dynamics was observed for diatomic chain. In Fig. 2, we present the time evolution of L_k for the case of $\varepsilon=1/10$, $A=0.02$, $\delta=0$, and different N: (a) $N=24$, (b) $N=26$, (c) $N=28$, and (d) $N=52$. We found that for $N\leq 24$, the modulational instability does not manifest itself [see panel (a)] while it does for $N\geq 26$ [see panels (b)–(d)]. This fact suggests that only sufficiently long waves are modulationally unstable. Let us denote as N^* the longest chain showing stable dynamics (e.g., for the case presented in Fig. 1, $N^*=26$). We have done similar simulations for

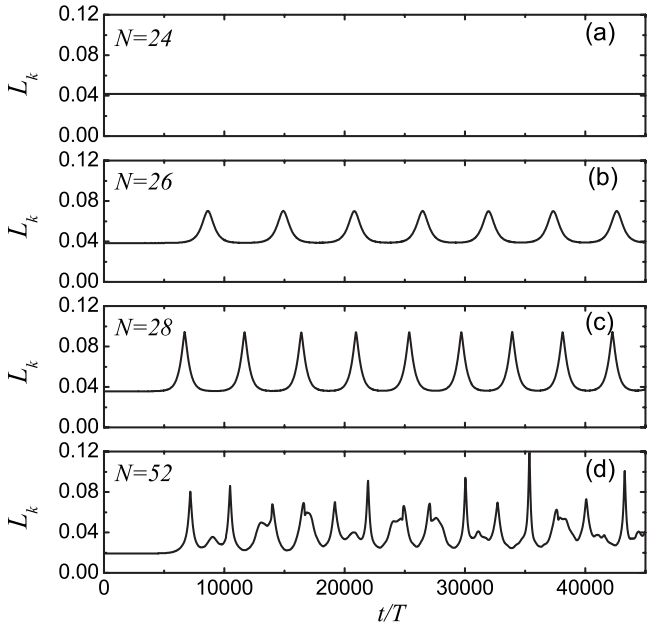

FIG. 2. Time evolution of L_k in the diatomic chain with $\varepsilon=1/10$ for different N as indicated in each panel. Here $A=0.02$ and $\delta=0$.

various A and found that N^* is proportional to $1/A$. If the length of the chain lies in the range of $N^*-1.5N^*$, then L_k is a nearly periodic function of time [see panels (b) and (c)], while for longer chains L_k, varies with time aperiodically [see panel (d) where the length of the chain is nearly equal to $2N^*$]. This is understandable because for long chains, the unstable dynamics is governed by a superposition of a number of unstable waves. We do not present the time evolution of k and K for the graphs of Fig. 2 because they are practically constant within the studied time domain being equal to $k=2\times10^{-4}$ and $K=0$. Thus, the kinetic energy of the light atoms is not given to the heavy atoms and the latter ones remain practically motionless even in the regime of modulationally unstable dynamics. This behavior contrasts to the case of the monatomic chain, shown in Fig. 1, where odd and even sublattices periodically exchange by their kinetic energies but L_k and L_K remain practically constant.

Careful look at the panels (b)–(d) of Fig. 2 reveals that L_k starts to oscillate after a time delay which increases with decrease in the initial perturbation Δ_n. On the other hand, we found that for small Δ_n, the period of L_k is *not* sensitive to the magnitude of Δ_n.

In Fig. 3, we give another presentation of the data obtained in the numerical run presented in Fig. 2(c). Here we show (a) particles on the $(n,t/T)$ plane with $k_n>3\times10^{-4}$ and (b) values of k_n for the particles of the chain at the three values of time indicated in (a) as 1, 2, and 3. One can see that, in this case (and, more generally, in the case when the length of the chain lies in the range of $N^*-1.5N^*$, as it was already mentioned), the kinetic energy of light particles localizes and delocalizes almost periodically in time and space.

C. Analytical treatment for $\varepsilon=1$

For $\varepsilon=1$, the equations of motion Eq. (14) under the symmetry constrains $v_n=-v_{n+1}=v$, $V_n=-V_{n+1}=V$ reduce to

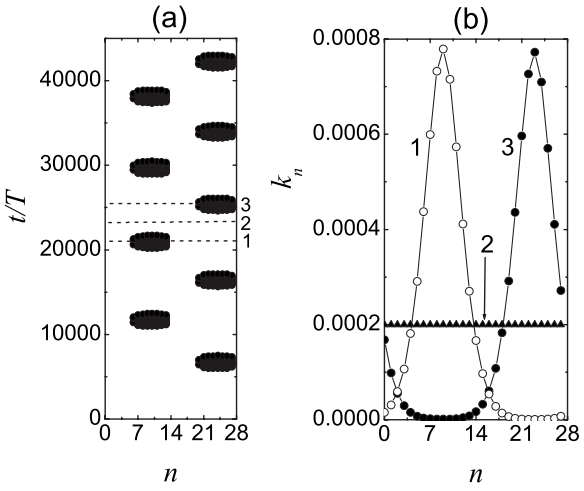

FIG. 3. (a) Plot showing particles with $k_n>3\times10^{-4}$ on the $(n,t/T)$ plane. (b) Values of k_n for the particles of the chain at the three values of time indicated in (a) as 1, 2, and 3. This is a different presentation of the data obtained in the numerical run presented in Fig. 2(c). Parameters: $A=0.02$, $\varepsilon=1/10$, $N=28$, and $\delta=0$.

$$\ddot{v}=-\omega^2 v+4\beta v V,$$

$$\ddot{V}=-\omega^2 V-4\beta v V, \tag{20}$$

where we have used Eq. (18). Initial conditions for Eq. (20) will be set assuming that the particles move as follows:

$$v(t)=A\sin(\omega t),$$

$$V(t)=B\sin(\omega t), \tag{21}$$

i.e., we set $v(0)=V(0)=0$, $\dot{v}(0)=A\omega$, and $\dot{V}(0)=B\omega$. Note that for $B=0$, Eq. (21) is a solution to Eq. (20). We will always take $B\ll A$ when Eq. (21) can be viewed as an approximate solution to Eq. (20).

In terms of new variables

$$\eta=v+V,\quad \mu=v-V, \tag{22}$$

Eq. (20) can be written as

$$\ddot{\eta}=-\omega^2\eta,$$

$$\ddot{\mu}=-\omega^2\mu+2\beta(\eta^2-\mu^2). \tag{23}$$

Due to the possibility of the time shift, solution to the first equation in Eq. (23) can be taken as follows:

$$\eta=C\sin(\omega t), \tag{24}$$

where C is the integration constant and then the second equation assumes the form

$$\ddot{\mu}=-\omega^2\mu+2\beta[C^2\sin^2(\omega t)-\mu^2]. \tag{25}$$

Let us look for the solution to Eq. (25) of the form

$$\mu=a_0+a_{1s}\sin(\omega t)+a_{1c}\cos(\omega t)+a_{2s}\sin(2\omega t)+a_{2c}\cos(2\omega t), \tag{26}$$

where it is assumed that the amplitudes vary slowly with

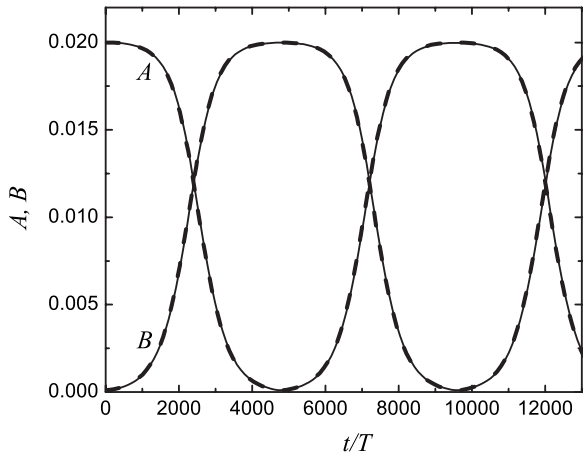

FIG. 4. Comparison of the results of numerical integration of Eq. (20) for rapidly changing variable (solid lines) and Eq. (27) for slow amplitudes (dashed lines). Amplitudes A and B of the two particles are shown as the functions of dimensionless time t/T, where T is the period of fast oscillations. Model parameters: $\omega^2=2$, $\beta=3/2$. Initial condition parameters: $A=0.02$, $B=10^{-4}$, $C=A+B=0.0201$, $a_{1s}(0)=A-B=0.0199$, and $a_{1c}(0)=0$.

time and $a_0(t), a_{2s}(t), a_{2c}(t) \ll a_{1s}(t), a_{1c}(t)$. Substituting Eq. (26) into Eq. (25) and equalizing the coefficients in front of similar terms, one finds $a_0=(\beta/\omega^2)(C^2-a_{1s}^2-a_{1c}^2)$, $a_{2s}=(2\beta/3\omega^2)a_{1s}a_{1c}$, $a_{2c}=(\beta/3\omega^2)(C^2-a_{1s}^2+a_{1c}^2)$, and obtains the following set of equations for the slowly varying main amplitudes:

$$\dot{a}_{1s}=-\frac{5\beta^2}{3\omega^3}\left(\frac{7}{5}C^2-a_{1s}^2-a_{1c}^2\right)a_{1c},$$

$$\dot{a}_{1c}=\frac{5\beta^2}{3\omega^3}(C^2-a_{1s}^2-a_{1c}^2)a_{1s}. \tag{27}$$

First of all, let us compare the results of numerical integration of Eqs. (20) and (27). To do so, we need to set the initial conditions for Eq. (27) equivalent to the initial conditions Eq. (21) for Eq. (20) and also we need to express the amplitude C in terms of the amplitudes A and B. Inserting Eqs. (21) and (24), and the main part of Eq. (26) (i.e., at $a_0=a_{2s}=a_{2c}=0$) into Eq. (22), we find the necessary relations $C=A+B$, $a_{1s}(0)=A-B$, and $a_{1c}(0)=0$.

The result of comparison is presented in Fig. 4 for $A=0.02$, $B=10^{-4}$, and hence for $C=A+B=0.0201$, $a_{1s}(0)=A-B=0.0199$, and $a_{1c}(0)=0$. For the initial value problem expressed by Eqs. (20) and (21), we plot the time variation of the amplitudes $A(t)$ and $B(t)$ of the rapidly oscillating variables $v(t)$ and $V(t)$ (solid lines), while for Eq. (27), we plot (by the dashed lines) the amplitudes of the two particles that can be approximately expressed through the main amplitudes as follows: $A(t)=\sqrt{A_s^2+A_c^2}$, $B(t)=\sqrt{B_s^2+B_c^2}$, where $A_s(t)=[C+a_{1s}(t)]/2$, $A_c(t)=a_{1c}(t)/2$, $B_s(t)=[C-a_{1s}(t)]/2$, and $B_c(t)=-a_{1c}(t)/2$.

One can see from Fig. 4 that the result of integration of Eq. (27) for slow amplitudes gives a very good fit of the result obtained by integration of Eq. (20) for the rapidly changing variables $v(t)$ and $V(t)$.

In order to investigate Eq. (27), we introduce the following dimensionless variables:

$$\tau=\frac{5\beta^2C^2}{3\omega^3}t, \quad a_{1s}(t)=Cx(\tau), \quad a_{1c}(t)=Cy(\tau), \tag{28}$$

and get

$$\dot{x}=-\left(\frac{7}{5}-x^2-y^2\right)y,$$

$$\dot{y}=(1-x^2-y^2)x. \tag{29}$$

Equation for the integral curves,

$$\frac{dy}{dx}=-\frac{(1-x^2-y^2)x}{(7/5-x^2-y^2)y}, \tag{30}$$

can be solved to give

$$\left(x^2+y^2-\frac{7}{5}\right)^2+\frac{4}{5}x^2=c^2, \tag{31}$$

with c being the integration constant, and using this relation, one can express the solution in the following parametric form:

$$x=\frac{\sqrt{5}}{2}c\cos\phi,$$

$$y_{1,2}=\pm\sqrt{\frac{7}{5}+c\sin\phi-\frac{5}{4}c^2\cos^2\phi}. \tag{32}$$

Substituting Eq. (32) into Eq. (29), one obtains equation for $\phi(\tau)$ which, for the case of small amplitudes ($a \ll 1$), has the following solution:

$$\phi(\tau)\approx\frac{2\sqrt{7}}{5}\tau+\frac{5c}{7}\sin^2\frac{\sqrt{7}\tau}{5}. \tag{33}$$

Zero-order approximation with respect to the amplitude c gives the period of $x(t)$ equal to $5\pi/\sqrt{7}$ in terms of time τ, which, in terms of time t, becomes

$$S\approx\frac{3\pi}{\sqrt{7}}\frac{\omega^3}{\beta^2C^2}. \tag{34}$$

Thus, we have $S\sim C^{-2}$ and this explains the results presented in Fig. 1, where one can see that the period of energy exchange between sublattices of even and odd particles, S, is proportional to A^{-2}, where A is the amplitude of the mode Eq. (17) excited at $t=0$ (the role of A is played by C in this section).

III. BREATHERS AND ENERGY LOCALIZATION IN TWO-DIMENSIONAL DIATOMIC LATTICES

A. Numerical approach

As a more general discrete nonlinear system of higher dimension, we consider a hypothetic two-dimensional (2D) crystal of E_3F stoichiometry. We assume that the atoms oc-

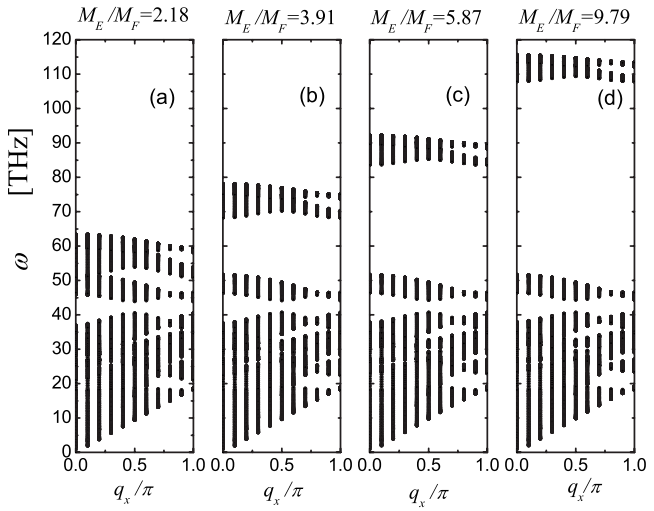

FIG. 5. Phonon spectra for the 2D diatomic crystal with the mass ratios M_E/M_F equal to (a) 2.18, (b) 3.91, (c) 5.87, and (d) 9.79. Width of the gap in the phonon spectrum increases with increase in M_E/M_F.

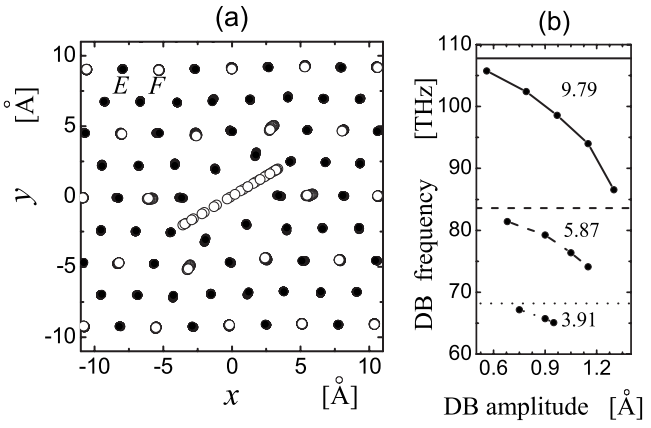

FIG. 6. (a) Stroboscopic picture presenting dynamics of atoms in the vicinity of DB in the 2D crystal with the mass ratio M_E/M_F=9.79. Heavy (light) atoms are shown by dots (open circles). Displacements of the atoms are multiplied by factor 4. (b) DB frequency as the function of DB amplitude for M_E/M_F=3.91, 5.87, and 9.79 with numerical points connected by the dotted, dashed, and solid lines, respectively. The horizontal lines of similar type show for each case the upper edge of the phonon gap (cf. Fig. 5).

cupy the points of the 2D hexagonal lattice [(111) plane of a fcc crystal] generated by the vectors $(a,0)$, $(a/2,\sqrt{3}a/2)$, where a is the lattice parameter. The atoms inside the computational cell, subjected to periodic boundary conditions, are numbered by the three indices m,n,i, where $1 \le m$, $n \le 32$ specifies the number of primitive cell, and $1 \le i \le 4$ specifies the number of atom inside a primitive cell. The primitive cell of the superstructure is generated by the vectors $(2a,0)$, $(a,\sqrt{3}a)$. It contains three atoms of sort E with the sublattice shift vectors (0,0), $(a,0)$, $(a/2,\sqrt{3}a/2)$, and one atom of sort F with the sublattice shift vector $(3a/2,\sqrt{3}a/2)$.

The atoms interact by means of the Morse interatomic potentials

$$U_{KL}(r) = D_{KL}\beta_{KL}e^{-\alpha_{KL}r}[\beta_{KL}e^{-\alpha_{KL}r} - 2], \qquad (35)$$

where r is the distance between considered pair of atoms, $K,L=\{E,F\}$, and we took the following parameters: α_{EE} =1.36605 Å^{-1}, β_{EE}=41.0494, D_{EE}=0.470513 eV, α_{FF} =1.02658 Å^{-1}, β_{FF}=27.4979, D_{FF}=0.318004 eV, α_{EF} =1.16809 Å^{-1}, β_{EF}=27.1260, and D_{EF}=0.4995026 eV. These parameters correspond to Ni_3Al alloy. For the cutoff radius of 16 Å, the equilibrium lattice parameter was found to be a=2.6 Å. For the mass of atom of sort E, we took the mass of Ni atom which is equal to M_E=58.71 g/mol. For the mass of atom of sort F, we took four different values: $M_F=M_E/2.18$, $M_F=M_E/3.91$, $M_F=M_E/5.87$, and $M_F=M_E/9.79$. Note that the first value corresponds to the actual mass of Al atom (26.981 g/mol), while in the other cases M_F is smaller than Al atom mass.

Equations of motion for the atoms were solved numerically by the Störmer method of order 6. Size and shape of the computational cell did not change with time.

B. Discrete breathers

In Figs. 5(a)–5(d), we present the phonon spectra of the considered 2D diatomic crystal for the four different mass ratios M_E/M_F=2.18, 3.91, 5.87, and 9.79, respectively. Phonon frequencies were calculated for the points of the first Brillouin zone $(q_x,q_y)=(k\pi/10,l\pi/10)$ with $0 \le k$, $l \le 10$ and projected on the (q_x,ω) plane. One can see that the width of the gap in the phonon spectrum increases together with the mass ratio M_E/M_F.

We were unable to excite DBs with frequencies above the phonon spectrum for any of the considered mass ratios M_E/M_F. For the mass ratio M_E/M_F=2.18, the gap is too narrow to support a gap DB. On the other hand, for the mass ratios $M_E/M_F > 3.5$, the gap DBs can be easily excited by setting for one light atom a large initial deviation (of order of lattice parameter a) with all other atoms being at their lattice positions and with all atoms having zero initial velocities. DB is formed after a transient period when a portion of energy of the initial excitation spreads over the crystal in the form of small-amplitude vibrations. Then one can obtain the results presented in Fig. 6(b) by measuring the amplitude and the frequency of DB.

In Fig. 6(a), the stroboscopic picture presents dynamics of atoms in the vicinity of DB in the crystal with the mass ratio M_E/M_F=9.79. Heavy (light) atoms are shown by dots (open circles). Displacements of the atoms are multiplied by factor 4. It is clear that the DB is highly localized and only one light atom oscillates with a very large amplitude (we note that the degree of localization decreases with decrease in M_E/M_F).

In Fig. 6(b), we show the frequency of DB as the function of its amplitude for M_E/M_F=3.91, 5.87, and 9.79, connecting the numerical points by the dotted, dashed, and solid lines, respectively. The horizontal lines of similar type show for each case the upper edge of the phonon gap (cf. Fig. 5). It can be seen that frequencies of the DBs lay in the gap of the phonon band and, for this reason, they practically do not

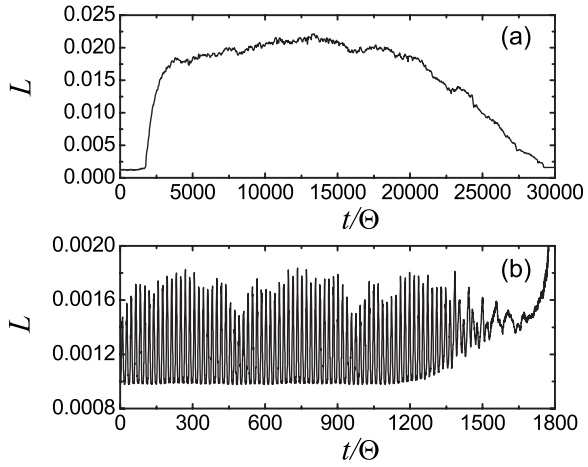

FIG. 7. Localization parameter L as the function of dimensionless time t/Θ, where Θ is the period of DB. Panel (b) shows in a different scale the portion of panel (a) for small t/Θ. Results for the mass ratio $M_E/M_F=9.79$ and the amplitude of the initially excited plane mode $A=0.038a$.

excite phonon modes and oscillate for a very long time radiating no energy. DB frequency decreases with increase in its amplitude meaning that crystals with the Morse interatomic potentials effectively exhibit soft anharmonicity and this explains why we could not obtain DBs with frequencies above the phonon spectrum.

C. Anti-FPU energy localization

The Brillouin-zone-edge mode in the 2D crystal was excited as follows. Light atoms (of sort F) in the primitive cells with odd $m+n$ were shifted away from their equilibrium positions in x direction by A, while the ones with even $m+n$ by $-A$. Heavy atoms (of sort E) were not shifted from their lattice positions and initial velocities of all atoms were zero. For the mode amplitude, A, we set rather small values $A=\{0.077a, 0.058a, 0.038a\}$. The excited mode was found to be unstable.

We calculated the localization parameter

$$L=\frac{\sum_{m,n=1}^{32}\langle E_{m,n}\rangle^2}{\left(\sum_{m,n=1}^{32}\langle E_{m,n}\rangle\right)^2}, \tag{36}$$

where $\langle E_{m,n}\rangle$ is the averaged over period of DB total energy of the light atom in the (m,n)th primitive cell (heavy atoms were not taken into account in the calculation of L).

In Fig. 7, for the case of $M_E/M_F=9.79$ and $A=0.038a$, we give L as the function of dimensionless time t/Θ, where Θ is the period of DB. Panel (b) shows in a different scale the portion of panel (a) for small t/Θ. In the time evolution of L, one can see several stages. During the first stage [shown also in panel (b)], L remains small oscillating with the period approximately equal to 20Θ. Analysis of the atomic displacements revealed that the oscillation of L at this stage is related to the modulational instability of the initially excited wave

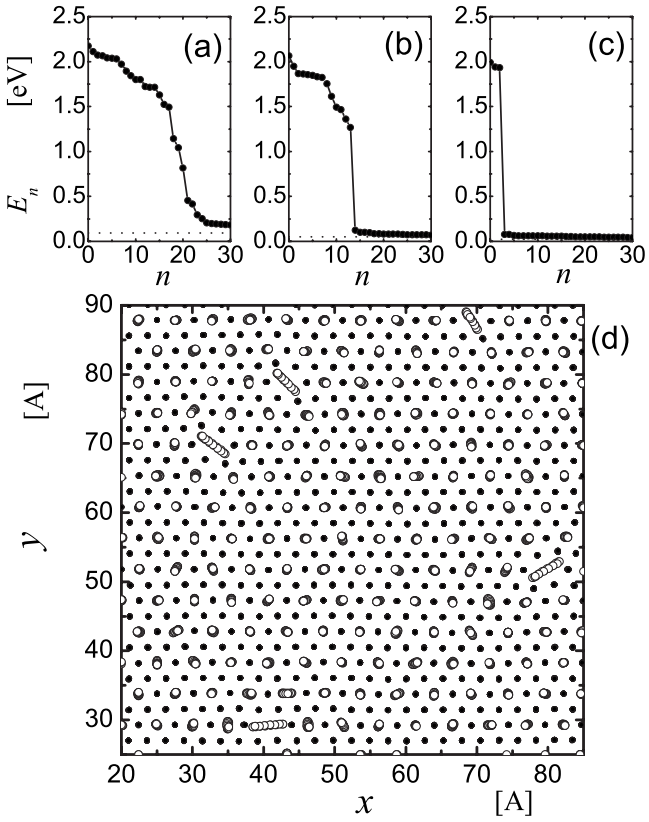

FIG. 8. Total energies of the light atoms averaged over Θ, $\langle E_n\rangle$, sorted by decrease of $\langle E_n\rangle$ for the case of $M_E/M_F=9.79$ and (a) $A=0.077a$, (b) $A=0.058a$, and (c) $A=0.038a$. These results were obtained at the time when L reaches its maximum. Horizontal dashed lines at the bottom of each panel show the energies of light atoms in the initially excited plane wave. Atoms having large energies $\langle E_n\rangle$ correspond to DBs. (d) A part of the periodic computational cell showing multiple excitation of BDs for the case presented in (a). Heavy (light) atoms are shown by dots (open circles). Displacements of the atoms are multiplied by factor 2.

with respect to relatively long wave. The instability results in the periodic in time and space energy localizations/delocalizations similar to that described in Sec. II in frame of the one-dimensional (1D) diatomic crystal. The first stage ends by a significant growth of L (by 1 order of magnitude) and during the second stage L remains large and nearly constant for a long time (of order of $10^4\Theta$). Analysis of the atomic displacements showed that at the second stage, a few DBs with very large amplitudes [similar to those shown in Fig. 6(a)] are formed and they accumulate a good portion of the energy of the initially excited wave. At the third stage, L decreases and the fourth stage corresponds to thermal equilibrium with constant L being nearly as small as at the first stage. For the case of $M_E/M_F=9.79$, we have analyzed the effect of the amplitude of the initially excited mode, A, and found that for smaller A, the duration of the second stage with large L is longer and the maximum value of L is larger.

In Fig. 8, we present the total energies of the light atoms averaged over Θ, $\langle E_n\rangle$, sorted by decrease of $\langle E_n\rangle$ for the case of $M_E/M_F=9.79$ and (a) $A=0.077a$, (b) $A=0.058a$, and (c) $A=0.038a$. These results were obtained at the time when

L reaches its maximum. Horizontal dashed lines at the bottom of each panel show the energies of light atoms in the initially excited plane wave. Atoms having large energies $\langle E_n \rangle$ correspond to DBs. Maximum energy of DB is equal to about 2 eV and this energy does not depend on A. The number of DBs formed in the computational cell increases with A. Thus, in (a) there are about 20 DBs, in (b) 14 DBs, and in (c) only 3 DBs. In (d), we show a part of the periodic computational cell where multiple excitation of BDs can be seen for the case presented in (a). Heavy (light) atoms are shown by dots (open circles). Displacements of the atoms are multiplied by factor 2.

IV. SUMMARY AND CONCLUSIONS

We have analyzed the dynamics of one- and two-dimensional diatomic lattices with the atoms interacting via Morse potentials. First, we have studied numerically modulational instability in one-dimensional diatomic lattices starting from the staggered state at the edge of the Brillouin zone (the so-called anti-FPU problem). Our numerical results demonstrate that the wavelength of the shortest unstable wave, λ^*, is scaled as $\lambda^* \sim A^{-1}$, where A is the amplitude of the initially excited edge mode. We have found that in this anti-FPU case, the speed of thermalization of the chain is sensitive to the length of the chain and the wavelength λ^*. If the length of the chain (subjected to the periodic boundary conditions) is smaller than $\lambda^*/2$, a stable dynamics is observed with *no energy exchange* between the modes. For the chains with the length ranging from $\lambda^*/2$ to $(3/4)\lambda^*$, we have observed periodic in time spatial energy localization that happens for extremely long time without noticeable thermalization of the chain. The period of the periodic energy localization/delocalization is proportional to A^{-2}. For the chains with the length larger than $(3/4)\lambda^*$, the energy localization becomes aperiodic both in time and space and thermalization of the chain goes faster.

We have studied the effect of the mass ratio $\varepsilon = m/M$, $m \leq M$, on the unstable dynamics of the system. We have found that λ^* grows with ε and for the limiting case of equal masses ($\varepsilon = 1$), one has $\lambda^* \to \infty$. In this case, no spatial energy localization has been noticed but instead, we have observed the periodic energy exchange between sublattices of odd and even particles. Period of the energy exchange S has been found to be proportional to A^{-2} and this has been confirmed by the analytical solution obtained for the case of $\varepsilon = 1$.

In the case of two-dimensional diatomic lattices, we have used the Morse potentials taking into account the long-range interactions. A gap in the phonon spectrum appears for sufficiently large mass ratio M_E/M_F. For $M_E/M_F \geq 3.5$, the gap discrete breathers can be easily excited. Note that experimentally gap DBs were observed in NaI with the mass ratio $M_I/M_{Na} = 5.52$.[18] We have also found that the DB frequency decreases with increase in its amplitude so that the Morse potentials, with the long-range interactions taken into account, result in soft anharmonicity. This fact suggests that in the lattices with the Morse interactions (1D or 2D), it is unlikely to find DBs with the frequencies above the phonon spectrum. Thus, the discrete breathers can be expected only in the lattices with a gap in the phonon spectrum and this may happen for the crystals with a complex structure.

Finally, we have studied numerically the energy localization phenomenon in the two-dimensional diatomic lattices via the evolution of modulationally unstable Brillouin-zone-edge mode excited in such a way that only light atoms are displaced initially whereas heavy atoms remain at rest. We have observed that, for sufficiently small amplitude of the staggered plane wave, a periodic in time spatial energy localization/delocalization at the earlier stage of the evolution of the unstable mode, similar to the case of one-dimensional lattices. At the later stage, we have observed the formation of a few highly localized, large-amplitude localized modes in the form of discrete breathers. Slow radiation of energy by the DBs at the final stage of the evolution results in the subsequent thermal equilibrium of the system.

ACKNOWLEDGMENTS

S.V.D. thanks the Nonlinear Physics Center at the Australian National University for warm hospitality during his visit to Canberra and acknowledges fruitful discussions with Andrey Miroshnichenko. S.V.D., I.A.M., and K.L.Z. gratefully acknowledge financial support provided by the DST-RFBR joint Grant No. 08-02-91316-Ind-a and the RFBR Grant No. 09-08-00696-a. This work was partially supported by the Australian Research Council.

[1] E. Fermi, J. Pasta, and S. Ulam, Los Alamos Science Laboratory Report No. LA-1940, 1955 (unpublished); Reprinted in *Collected Papers of Enrico Fermi*, edited by E. Segre (University of Chicago Press, Chicago, 1965), Vol. 2, p. 978.
[2] Chaos **15** (2005), special issue on the FPU problem.
[3] T. Dauxois, R. Khomeriki, F. Piazza, and S. Ruffo, Chaos **15**, 015110 (2005).
[4] A. J. Sievers and S. Takeno, Phys. Rev. Lett. **61**, 970 (1988).
[5] S. Flach and C. R. Willis, Phys. Rep. **295**, 181 (1998).
[6] S. Flach and A. V. Gorbach, Phys. Rep. **467**, 1 (2008).
[7] M. J. Ablowitz and B. M. Herbst, SIAM J. Appl. Math. **50**, 339 (1990).
[8] T. J. Alexander, E. A. Ostrovskaya, and Yu. S. Kivshar, Phys. Rev. Lett. **96**, 040401 (2006).
[9] E. V. Doktorov, V. M. Rothos, and Yu. S. Kivshar, Phys. Rev. A **76**, 013626 (2007).
[10] D. Hennig, S. Fugmann, L. Schimansky-Geier, and P. Hanggi, Phys. Rev. E **76**, 041110 (2007).
[11] A. Maluckov, Lj. Hadzievski, N. Lazarides, and G. P. Tsironis, Phys. Rev. E **79**, 025601(R) (2009).
[12] Y. Doi, A. Nakatani, and K. Yoshimura, Phys. Rev. E **79**, 026603 (2009).
[13] Yu. A. Kosevich and S. Lepri, Phys. Rev. B **61**, 299 (2000).
[14] A. V. Gorbach and M. Johansson, Phys. Rev. E **67**, 066608

(2003).
[15] G. James and M. Kastner, Nonlinearity **20**, 631 (2007).
[16] S. V. Dmitriev, N. N. Medvedev, R. R. Mulyukov, O. V. Pozhidaeva, A. I. Potekaev, and M. D. Starostenkov, Russ. Phys. J. **51**, 858 (2008).
[17] D. K. Campbell, S. Flach, and Yu. S. Kivshar, Phys. Today **57**(1), 43 (2004).
[18] M. E. Manley, A. J. Sievers, J. W. Lynn, S. A. Kiselev, N. I. Agladze, Y. Chen, A. Llobet, and A. Alatas, Phys. Rev. B **79**, 134304 (2009).
[19] M. E. Manley, arXiv:0905.2988 (unpublished).
[20] D. C. Rapaport, *The Art of Molecular Dynamics Simulation* (Cambridge University Press, Cambridge, England, 1996).
[21] T. Niiyama, Y. Shimizu, T. R. Kobayashi, T. Okushima, and K. S. Ikeda, Phys. Rev. E **79**, 051101 (2009); N. D. Afify and G. Mountjoy, Phys. Rev. B **79**, 024202 (2009); S. I. Lee and S. J. Lee, Phys. Rev. E **78**, 041504 (2008).
[22] T. Castan, A. Planes, A. Ramos, and J. Vinals, Phys. Rev. B **39**, 3551 (1989); B. K. Ray and G. D. Nigam, Phys. Status Solidi A **33**, K101 (2006); T. H. Fang, C.-D. Wu, and W.-J. Chang, Appl. Surf. Sci. **253**, 6963 (2007).